communications physics

ARTICLE

https://doi.org/10.1038/s42005-022-00804-7 OPEN

Anapole superconductivity from $\mathcal{PT}$-symmetric mixed-parity interband pairing

Shota Kanasugi [1]✉ & Youichi Yanase[1,2]✉

Recently, superconductivity with spontaneous time-reversal or parity symmetry breaking is attracting much attention owing to its exotic properties, such as nontrivial topology and nonreciprocal transport. Particularly fascinating phenomena are expected when the time-reversal and parity symmetry are simultaneously broken. This work shows that time-reversal symmetry-breaking mixed-parity superconducting states generally exhibit an unusual asymmetric Bogoliubov spectrum due to nonunitary interband pairing. For generic two-band models, we derive the necessary conditions for the asymmetric Bogoliubov spectrum. We also demonstrate that the asymmetric Bogoliubov quasiparticles lead to the effective anapole moment of the superconducting state, which stabilizes a nonuniform Fulde-Ferrell-Larkin-Ovchinnikov state at zero magnetic fields. The concept of anapole order employed in nuclear physics, magnetic materials science, strongly correlated electron systems, and optoelectronics is extended to superconductors by this work. Our conclusions are relevant for any multiband superconductors with competing even- and odd-parity pairing channels. Especially, we discuss the superconductivity in UTe_2.

[1] Department of Physics, Kyoto University, Kyoto 606-8502, Japan. [2] Institute for Molecular Science, Okazaki 444-8585, Japan.
✉email: kanasugi.shouta.62w@st.kyoto-u.ac.jp; yanase@scphys.kyoto-u.ac.jp

Parity symmetry ($\mathcal{P}$-symmetry) and time-reversal symmetry ($\mathcal{T}$-symmetry) are fundamental properties of quantum materials, such as insulators, metals, magnets, and superconductors. Superconductivity is caused by the quantum condensation of either even-parity or odd-parity Cooper pairs, which correspond to spin-singlet or spin-triplet superconductivity due to the fermion antisymmetry[1]. The order parameter of conventional superconductors breaks neither $\mathcal{P}$-symmetry nor $\mathcal{T}$-symmetry. However, competition and coexistence of multiple pairing instabilities lead to exotic superconductivity, such as chiral superconductivity with spontaneous $\mathcal{T}$-symmetry breaking[2] related to the nontrivial topology[3,4] and anomalous transport[5].

In particular, mixed-parity superconductivity with coexistent even- and odd-parity pairing channels has been widely discussed in noncentrosymmetric superconductors[6,7], ultracold fermion systems[8,9], and spin-orbit-coupled systems in the vicinity of the $\mathcal{P}$-symmetry broken phase[10–14]. The $\mathcal{P}$-symmetry is broken in such superconductors. Furthermore, spontaneous $\mathcal{T}$-symmetry breaking realized by the $\pm\pi/2$ phase difference between even- and odd-parity pairing potentials is energetically favored[15–17] (Fig. 1a), when the spin-orbit coupling (SOC) due to noncentrosymmetric crystal structure is absent or weak. This class of superconducting states spontaneously breaks both $\mathcal{P}$- and $\mathcal{T}$-symmetries but maintain the combined $\mathcal{PT}$-symmetry. There have been considerable interests in studying such $\mathcal{PT}$-symmetric mixed-parity superconductivity. The three-dimensional $s+ip$-wave superconductivity has attracted much theoretical attention as a superconducting analog of axion insulators[18–23]. The $\mathcal{PT}$-symmetric mixed-parity pairing has also been theoretically proposed in Sr_2RuO_4[24]. Furthermore, a mixed-parity superconducting state in UTe_2[25] has been predicted to explain experimentally-observed multiple superconducting phases[26–33].

In previous works, the mixed-parity superconductivity has been theoretically studied mainly in single-band models for spin-1/2 fermions[15,16,18–21,23]. On the other hand, it has recently been recognized that the multiband structure of the Cooper pair's wave function arising from internal electronic degrees of freedom (DOF) (e.g., orbital and sublattice) induces exotic superconducting phenomena. For instance, multiband superconductors have attracted much attention as a platform realizing odd-frequency pairing[34]. In $\mathcal{T}$-symmetry breaking superconductors, an intrinsic anomalous Hall effect emerges owing to the multiband nature of Cooper pairs[5,35–38]. In particular, even-parity $\mathcal{T}$-symmetry breaking superconductors host topologically protected Bogoliubov Fermi surfaces in the presence of interband pairing[39,40].

In this work, we show that $\mathcal{PT}$-symmetric mixed-parity superconducting states generally exhibit an asymmetric Bogoliubov spectrum (BS) in multiband systems, although it is overlooked in single-band models. We demonstrate that such asymmetric deformation of the BS is induced by a nonunitary interband pairing (see Fig. 1b), and derive the necessary conditions for generic two-band models. Although we consider two-band systems for simplicity throughout this paper, our theory is relevant for any multiband superconductors with multiple bands near the Fermi level. In addition, we show that the Bogoliubov quasiparticles with asymmetric BS stabilize the Fulde-Ferrell-Larkin-Ovchinnikov (FFLO) superconductivity[41,42], which is evident from the Lifshitz invariants[43], namely linear gradient terms, in the Ginzburg-Landau free energy. The Lifshitz

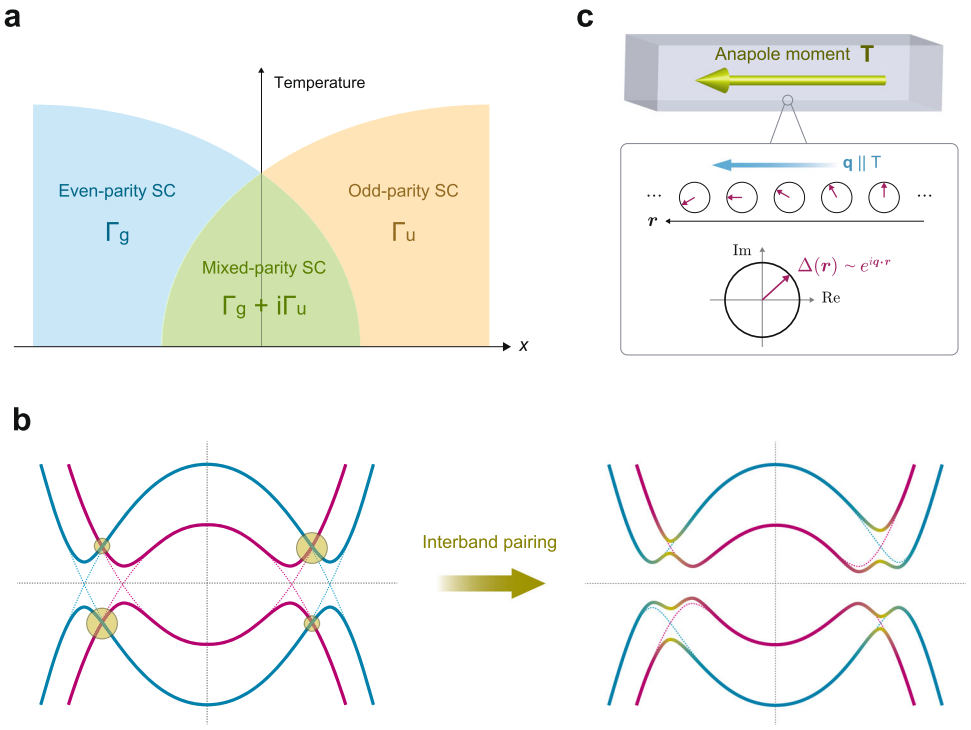

Fig. 1 Schematics of $\mathcal{PT}$-symmetric mixed-parity superconductivity (SC). a Schematic phase diagram in a superconductor with comparable strength of even- and odd-parity pairing interactions. The transition between the even-parity superconducting phase (Γ_g) and the odd-parity superconducting phase (Γ_u) is induced by tuning a control parameter x. For centrosymmetric systems with $\mathcal{T}$-symmetry, there is generally an intermediate mixed-parity superconducting phase ($\Gamma_g + i\Gamma_u$) where even- and odd-parity pairing components are coexistent with the relative phase difference $\pm\pi/2$. **b** Illustration for a mechanism of the asymmetric Bogoliubov spectrum (BS) in $\mathcal{PT}$-symmetric mixed-parity multiband superconductors. $\mathcal{P}$- and $\mathcal{T}$-symmetry breaking interband pairing induces an asymmetric modulation of the BS. **c** Schematic figure of the anapole superconducting states. In real space, the phase of the superconducting order parameter $\Delta(\mathbf{r})$ becomes nonuniform along a direction parallel to the effective anapole moment $\mathbf{T}$ as $\Delta(\mathbf{r}) \propto e^{i\mathbf{q}\cdot\mathbf{r}}$ with $\mathbf{q}\|\mathbf{T}$, where $\mathbf{q}$ is the center-of-mass momentum of Cooper pairs.

invariants are nonzero only for the anapole superconducting states, whose order parameters are equivalent to an anapole (magnetic toroidal) moment, namely a polar and time-reversal odd multipole[44], from the viewpoint of symmetry. It is shown that the phase of the superconducting order parameter is spatially modulated along the effective anapole moment of the superconducting state (see Fig. 1c). The concept of anapole order has been employed in nuclear physics[45], magnetic materials science[44], strongly correlated electron systems[46,47], and optoelectronics[48,49], and it is extended to superconductors by this work. In previous works, the FFLO superconductivity has been proposed in the presence of an external magnetic field[41–43,50] or coexistent magnetic multipole order[51,52]. However, the magnetic field causes superconducting vortices, prohibiting pure FFLO states, and the proposed multipole superconducting state has not been established in condensed matters. In contrast, the anapole superconductivity realizes the FFLO state without the aid of any other perturbation or electronic order. Note that an intrinsic nonuniform superconducting state has also been discussed in the Bogoliubov Fermi surface states[53], although its mechanism and symmetry are different from those of the anapole FFLO state.

Based on the obtained results, we predict the possible asymmetric BS and anapole superconductivity in UTe_2, a recently-discovered candidate of a spin-triplet superconductor[54]. The multiple pairing instabilities[26–33] and $\mathcal{T}$-symmetry breaking[55–58] were recently observed there.

Results

General two-band Bogoliubov-de Gennes Hamiltonian. We begin our discussion by considering the general form of the Bogoliubov-de Gennes (BdG) Hamiltonian for two-band systems:

$$\mathcal{H}=\frac{1}{2}\sum_{\mathbf{k}}(\hat{c}_{\mathbf{k}}^{\dagger},\hat{c}_{-\mathbf{k}}^{\mathrm{T}})\begin{pmatrix}H_0(\mathbf{k}) & \Delta(\mathbf{k})\\ \Delta^{\dagger}(\mathbf{k}) & -H_0^{*}(-\mathbf{k})\end{pmatrix}\begin{pmatrix}\hat{c}_{\mathbf{k}}\\ \hat{c}_{-\mathbf{k}}^{*}\end{pmatrix}, \tag{1}$$

where $\hat{c}_{\mathbf{k}}^{\mathrm{T}}=(c_{\mathbf{k}1\uparrow},c_{\mathbf{k}1\downarrow},c_{\mathbf{k}2\uparrow},c_{\mathbf{k}2\downarrow})$ is a spinor encoding the four internal electronic DOF stem from spin-1/2 and extra two-valued DOF, such as orbitals and sublattices. Then, the 4×4 matrices $H_0(\mathbf{k})$ and $\Delta(\mathbf{k})$ can be generally expressed as a linear combination of $\sigma_\mu\otimes\tau_\nu$ matrices, where σ_μ and τ_ν ($\mu,\nu=0,x,y,z$) are the Pauli matrices for the spin and extra DOF, respectively. However, we here introduce a more convenient form of the two-band BdG Hamiltonian using the Euclidean Dirac matrices γ_n ($n=1,2,3,4,5$), which satisfy $\{\gamma_m,\gamma_n\}=2\delta_{mn}$. See "Methods" for the correspondence between the $\sigma_\mu\otimes\tau_\nu$ and Dirac matrices. Assuming that the normal state preserves both $\mathcal{P}$- and $\mathcal{T}$-symmetries, the general form of the normal state Hamiltonian $H_0(\mathbf{k})$ can be expressed as

$$H_0(\mathbf{k})=(\epsilon_{\mathbf{k}}^0-\mu)\mathbf{1}_4+\boldsymbol{\epsilon}_{\mathbf{k}}\cdot\boldsymbol{\gamma}, \tag{2}$$

where $\mathbf{1}_4$ is the 4×4 unit matrix, $\boldsymbol{\gamma}=(\gamma_1,\gamma_2,\gamma_3,\gamma_4,\gamma_5)$ is the vector of the five Dirac matrices, $\epsilon_{\mathbf{k}}^0$ and $\boldsymbol{\epsilon}_{\mathbf{k}}=(\epsilon_{\mathbf{k}}^1,\epsilon_{\mathbf{k}}^2,\epsilon_{\mathbf{k}}^3,\epsilon_{\mathbf{k}}^4,\epsilon_{\mathbf{k}}^5)$ are the real-valued coefficients of these matrices, and μ is the chemical potential. Whereas $\epsilon_{\mathbf{k}}^0$ is an even function of momentum, $\mathbf{k}$-parity of other coefficients $\epsilon_{\mathbf{k}}^n$ ($n>0$) depends on the details of the extra DOF. The superconducting state is assumed to be a mixture of even- and odd-parity pairing components. The pairing potential $\Delta(\mathbf{k})$ for such mixed-parity superconducting states has the general form

$$\hat{\Delta}(\mathbf{k})=\Delta_1(\eta_{\mathbf{k}}^0\mathbf{1}_4+\boldsymbol{\eta}_{\mathbf{k}}\cdot\boldsymbol{\gamma})+\Delta_2\sum_{m<n}\eta_{\mathbf{k}}^{mn}i\gamma_m\gamma_n, \tag{3}$$

where $\hat{\Delta}(\mathbf{k})\equiv\Delta(\mathbf{k})U_{\mathrm{T}}^{\dagger}$ and U_{T} is the unitary part of the time-reversal operator. The complex-valued constants Δ_1 and Δ_2 represent the superconducting order parameters for the even- and odd-parity pairing channels, respectively. As a consequence of the fermionic antisymmetry $\Delta(\mathbf{k})=-\Delta^{\mathrm{T}}(-\mathbf{k})$, the even-parity (odd-parity) part of $\hat{\Delta}(\mathbf{k})$ is expressed by a linear combination of $\mathbf{1}_4$ and γ_n ($i\gamma_m\gamma_n$) as shown in Eq. (3) (see "Methods"). The real-valued functions $\eta_{\mathbf{k}}^0$, $\boldsymbol{\eta}_{\mathbf{k}}=(\eta_{\mathbf{k}}^1,\eta_{\mathbf{k}}^2,\eta_{\mathbf{k}}^3,\eta_{\mathbf{k}}^4,\eta_{\mathbf{k}}^5)$, and $\eta_{\mathbf{k}}^{mn}$ ($1\le m<n\le5$) determine the details of order parameters. Whereas $\eta_{\mathbf{k}}^0$ is an even function of momentum, $\mathbf{k}$-parity of others $\eta_{\mathbf{k}}^n$ and $\eta_{\mathbf{k}}^{mn}$ depends on the details of the extra DOF. Note that the $\mathbf{k}$-parity of $\eta_{\mathbf{k}}^n$ must be the same as that of $\epsilon_{\mathbf{k}}^n$. Although we adopt a BCS-type description of superconductivity in this work, we consider that our argument is hardly affected by enhanced quantum fluctuations in low-dimensional systems when the long-range order occurs.

Asymmetric BS from $\mathcal{PT}$-symmetric mixed-parity interband pairing. We here consider general BdG Hamiltonian including more than two band models, and later focus on the two-band models. In the following, we assume that each band is weakly coupled and the intraband pairing is dominant compared to the interband pairing. In such situations, spontaneous $\mathcal{T}$-symmetry breaking with maintaining the $\mathcal{PT}$-symmetry is energetically favored in the mixed-parity superconducting states[15,16], and the symmetry of the superconducting order parameter becomes equivalent to that of odd-parity magnetic multipoles[44]. A characteristic feature of the odd-parity magnetic multipole ordered state is the asymmetric modulation of the band structure[51,52,59,60], which leads to peculiar nonequilibrium responses such as nonreciprocal transport[61], magnetopiezoelectric effect[62,63], and photocurrent generation[48,49]. Therefore, the appearance of the asymmetric BS is naturally expected in the $\mathcal{PT}$-symmetric mixed-parity superconductors. However, the asymmetric BS is not obtained in single-band models (see later discussions).

To induce such asymmetric modulation in the BS, effects of the $\mathcal{P}$- and $\mathcal{T}$-symmetry breaking in the particle-particle superconducting channel should be transferred into the particle-hole channel. This suggests that it is not sufficient to consider only the pairing potential $\Delta(\mathbf{k})$, since it is not gauge invariant. Instead of $\Delta(\mathbf{k})$ alone, we need to consider gauge-invariant bilinear products of $\Delta(\mathbf{k})$ and $\Delta^{\dagger}(\mathbf{k})$[36] in order to reveal conditions for realizing the asymmetric BS. Here, we focus on the simplest bilinear products, that is, $\Delta(\mathbf{k})\Delta^{\dagger}(\mathbf{k})$. The parity-odd and time-reversal-odd ($\mathcal{P},\mathcal{T}$-odd) part of this bilinear product is calculated as

$$M_{-}^{(1)}(\mathbf{k})=\frac{1}{2}\left([\hat{\Delta}^{\mathrm{g}}(\mathbf{k}),\hat{\Delta}^{\mathrm{u}\dagger}(\mathbf{k})]+[\hat{\Delta}^{\mathrm{u}}(\mathbf{k}),\hat{\Delta}^{\mathrm{g}\dagger}(\mathbf{k})]\right), \tag{4}$$

where $\hat{\Delta}^{\mathrm{g}}(\mathbf{k})$ and $\hat{\Delta}^{\mathrm{u}}(\mathbf{k})$ are the even- and odd-parity part of $\hat{\Delta}(\mathbf{k})$, respectively (see Supplementary Note 1 for the derivation of Eq. (4)). Owing to the gauge invariance and $\mathcal{P},\mathcal{T}$-odd behavior of $M_{-}^{(1)}(\mathbf{k})$, a nonzero $M_{-}^{(1)}(\mathbf{k})$ can be a measure of the $\mathcal{P}$- and $\mathcal{T}$-symmetry breaking in the particle-hole channel, which permits emergence of the asymmetric BS. Note that the pairing state must be nonunitary to induce a nonzero $M_{-}^{(1)}(\mathbf{k})$, since $M_{-}^{(1)}(\mathbf{k})=0$ when $\Delta(\mathbf{k})\Delta^{\dagger}(\mathbf{k})$ is proportional to the unit matrix. In analogy with the spin polarization of nonunitary spin-triplet superconducting states in spin-1/2 single-band models[1], the $\mathcal{P},\mathcal{T}$-odd bilinear product $M_{-}^{(1)}(\mathbf{k})$ can be interpreted as a polarization of an internal DOF in the superconducting state.

The emergence of a nonzero $\mathcal{P},\mathcal{T}$-odd bilinear product $M_{-}^{(1)}(\mathbf{k})$ requires the interband pairing. To see this, we consider the problem in the band basis. Since $H_0(\mathbf{k})$ is assumed to preserve the $\mathcal{P}$- and $\mathcal{T}$-symmetries, the energy eigenvalues are doubly degenerate and labeled by a pseudospin index. Especially, we choose the so-called manifestly covariant Bloch basis[10], in which the pseudospin index transforms like a true spin-1/2 under time-reversal and crystalline symmetry operations. In this basis, the

intraband pairing potential is generally expressed as $\Delta_{\mathbf{k}} = (\psi_{\mathbf{k}} + \mathbf{d}_{\mathbf{k}} \cdot \mathbf{s}) i s_y$, where $\mathbf{s} = (s_x, s_y, s_z)$ are Pauli matrices in pseudospin space. The complex-valued functions $\psi_{\mathbf{k}}$ and $\mathbf{d}_{\mathbf{k}}$ are even and odd functions of $\mathbf{k}$, respectively. Then, in the absence of the interband pairing, the multiband BdG Hamiltonian matrix reduces to a series of decoupled blocks describing spin-1/2 single-band superconductors. The bilinear product for this intraband pairing potential is obtained as $\Delta_{\mathbf{k}}\Delta_{\mathbf{k}}^{\dagger} = (|\psi_{\mathbf{k}}|^2 + |\mathbf{d}_{\mathbf{k}}|^2)\mathbf{1}_2 + 2\mathrm{Re}(\psi_{\mathbf{k}}\mathbf{d}_{\mathbf{k}}^*) \cdot \mathbf{s} + i(\mathbf{d}_{\mathbf{k}} \times \mathbf{d}_{\mathbf{k}}^*) \cdot \mathbf{s}$, and the second and third terms are nonunitary components that break $\mathcal{P}$- and $\mathcal{T}$-symmetries, respectively. Here, $\mathbf{1}_2$ is the 2×2 unit matrix. However, there appears no term breaking both $\mathcal{P}$- and $\mathcal{T}$-symmetries, and hence the $\mathcal{P}, \mathcal{T}$-odd bilinear product for this $\Delta_{\mathbf{k}}$ must vanish. This indicates that the interband pairing is necessary for a nonzero $\mathcal{P}, \mathcal{T}$-odd bilinear product $M_{-}^{(1)}(\mathbf{k})$, which is essential for realizing the asymmetric BS. This is also the reason the asymmetric BS is not obtained in single-band models.

The presence of interband pairing can be characterized by the so-called superconducting fitness $F(\mathbf{k})$, which is defined as $F(\mathbf{k})U_{\mathrm{T}} = H_0(\mathbf{k})\Delta(\mathbf{k}) - \Delta(\mathbf{k})H_0^*(-\mathbf{k})$[64,65]. Since a nonvanishing $F(\mathbf{k})F^{\dagger}(\mathbf{k})$ quantifies the strength of interband pairing by definition[64,65], its $\mathcal{P}, \mathcal{T}$-odd part should be nonzero to realize a nonvanishing $M_{-}^{(1)}(\mathbf{k})$. The $\mathcal{P}, \mathcal{T}$-odd part of $F(\mathbf{k})F^{\dagger}(\mathbf{k})$ is obtained as

$$M_{-}^{(2)}(\mathbf{k}) = \frac{1}{2}\left([F^{\mathrm{g}}(\mathbf{k}), F^{\mathrm{u}\dagger}(\mathbf{k})] + [F^{\mathrm{u}}(\mathbf{k}), F^{\mathrm{g}\dagger}(\mathbf{k})]\right), \tag{5}$$

where $F^{\mathrm{g}}(\mathbf{k})$ and $F^{\mathrm{u}}(\mathbf{k})$ are the even- and odd-parity part of $F(\mathbf{k})$, respectively. If the normal state preserves both $\mathcal{P}$- and $\mathcal{T}$-symmetries, they are obtained as $F^{\mathrm{g,u}}(\mathbf{k}) = [H_0(\mathbf{k}), \hat{\Delta}^{\mathrm{g,u}}(\mathbf{k})]$. Note that the $\mathcal{P}, \mathcal{T}$-odd part of $F(\mathbf{k})F^{\dagger}(\mathbf{k})$ can be extracted in the same way as $\Delta(\mathbf{k})\Delta^{\dagger}(\mathbf{k})$ [compare Eq. (5) with Eq. (4)], since the transformation of $F(\mathbf{k})F^{\dagger}(\mathbf{k})$ under space-inversion and time-reversal can be described in the same way as that of $\Delta(\mathbf{k})\Delta^{\dagger}(\mathbf{k})$. Based on Eq. (5), not only the pair potential $\Delta(\mathbf{k})$ but also the normal part $H_0(\mathbf{k})$ must satisfy a proper condition to realize $M_{-}^{(2)}(\mathbf{k}) \neq 0$ and asymmetric BS.

From the above discussions, we conclude that the necessary (but not sufficient) condition for the asymmetric BS can be written as $M_{-}^{(1)}(\mathbf{k}) \neq 0 \cap M_{-}^{(2)}(\mathbf{k}) \neq 0$, which implies the superconductivity-driven $\mathcal{P}$- and $\mathcal{T}$-symmetry breaking in the particle-hole channel. We here write down this necessary condition for the general two-band BdG Hamiltonian. By substituting Eqs. (2) and (3) to Eqs. (4) and (5), we obtain the $\mathcal{P}, \mathcal{T}$-odd bilinear products $M_{-}^{(1)}(\mathbf{k})$ and $M_{-}^{(2)}(\mathbf{k})$ as follows:

$$M_{-}^{(1)}(\mathbf{k}) = 2\mathrm{Im}(\Delta_1\Delta_2^*) \sum_{m<n} \eta_{\mathbf{k}}^{mn}(\eta_{\mathbf{k}}^{n}\gamma_m - \eta_{\mathbf{k}}^{m}\gamma_n), \tag{6}$$

$$M_{-}^{(2)}(\mathbf{k}) = \mathrm{Tr}[M_{-}^{(1)}(\mathbf{k})\tilde{H}_0(\mathbf{k})]\tilde{H}_0(\mathbf{k}), \tag{7}$$

where $\tilde{H}_0(\mathbf{k}) \equiv H_0(\mathbf{k}) - (\epsilon_{\mathbf{k}}^0 - \mu)\mathbf{1}_4$. We see that $M_{-}^{(1)}(\mathbf{k})$ appears inside the expression of $M_{-}^{(2)}(\mathbf{k})$, and hence the necessary condition for the asymmetric BS can be simplified as $\mathrm{Tr}[M_{-}^{(1)}(\mathbf{k})\tilde{H}_0(\mathbf{k})] \neq 0$ in two-band models. Note that it is not clear whether $M_{-}^{(2)}(\mathbf{k})$ can be written in terms of $M_{-}^{(1)}(\mathbf{k})$ in more than two band models since Eq. (7) is derived for the general two-band model by using the properties of Dirac matrices. From Eqs. (6) and (7), the necessary condition (i.e., $\mathrm{Tr}[M_{-}^{(1)}(\mathbf{k})\tilde{H}_0(\mathbf{k})] \neq 0$) can be summarized as following two criteria; (i) the relative phase difference between even- and odd-parity pairing potentials must be nonzero so that $\mathrm{Im}(\Delta_1\Delta_2^*) \neq 0$, and (ii) the BdG Hamiltonian must satisfy $\epsilon_{\mathbf{k}}^m\eta_{\mathbf{k}}^n\eta_{\mathbf{k}}^{mn} \neq 0$ or $\epsilon_{\mathbf{k}}^n\eta_{\mathbf{k}}^m\eta_{\mathbf{k}}^{mn} \neq 0$ for $1 \leq {}^{\exists}m < {}^{\exists}n \leq 5$. Interpretations of these requirements in the $\sigma_\mu \otimes \tau_\nu$ basis are shown in "Methods" section.

We now confirm that the asymmetric BS indeed appears when the above two criteria are fulfilled. A minimal two-band model satisfying the criterion (ii) can be obtained by substituting $\boldsymbol{\epsilon}_{\mathbf{k}} = r\epsilon_{\mathbf{k}}^a\mathbf{e}_a + (1-r)\epsilon_{\mathbf{k}}^b\mathbf{e}_b$, $\boldsymbol{\eta}_{\mathbf{k}} = (1-r)\eta_{\mathbf{k}}^a\mathbf{e}_a + r\eta_{\mathbf{k}}^b\mathbf{e}_b$, and $\eta_{\mathbf{k}}^{mn} = \delta_{ma}\delta_{nb}\eta_{\mathbf{k}}^{ab}$ into Eqs. (2) and (3). Here, a and b are specific integers satisfying $1 \leq a < b \leq 5$, $\mathbf{e}_n$ is the unit vector for the n-th component, and r takes the value either 0 or 1. Under this setup, we can analytically diagonalize the BdG Hamiltonian as $\mathrm{diag}(E_{\mathbf{k}}^{+}\mathbf{1}_2, E_{\mathbf{k}}^{-}\mathbf{1}_2, -E_{-\mathbf{k}}^{+}\mathbf{1}_2, -E_{-\mathbf{k}}^{-}\mathbf{1}_2)$. Based on the correspondence between the Dirac matrices and $\sigma_\mu \otimes \tau_\nu$ matrices the energy spectrum $E_{\mathbf{k}}^{\pm}$ can be obtained as

$$E_{\mathbf{k}}^{\pm} = \sqrt{\xi_{\mathbf{k}}^2 + \frac{1}{4}\mathrm{Tr}\left[\Delta(\mathbf{k})\Delta^{\dagger}(\mathbf{k}) \pm \frac{M_{-}^{(1)}(\mathbf{k})\tilde{H}_0(\mathbf{k})}{r\epsilon_{\mathbf{k}}^a + (1-r)\epsilon_{\mathbf{k}}^b}\right]} \pm [r\epsilon_{\mathbf{k}}^a + (1-r)\epsilon_{\mathbf{k}}^b], \tag{8}$$

where $\xi_{\mathbf{k}} \equiv \epsilon_{\mathbf{k}}^0 - \mu$. By using the transformation properties of the BdG Hamiltonian under space-inversion and time-reversal, we can confirm that Eq. (8) satisfies $E_{-\mathbf{k}}^{+} \neq E_{\mathbf{k}}^{\pm}$ and $E_{-\mathbf{k}}^{-} \neq E_{\mathbf{k}}^{\pm}$ (i.e., the BS is asymmetric) when $\mathrm{Tr}[M_{-}^{(1)}(\mathbf{k})\tilde{H}_0(\mathbf{k})] \neq 0$. See "Methods" for the proof. This implies that $M_{-}^{(1)}(\mathbf{k}) \neq 0 \cap M_{-}^{(2)}(\mathbf{k}) \neq 0$ is indeed a necessary condition of the asymmetric BS.

Lifshitz invariants and effective anapole moment. To obtain further insight into the asymmetric BS, we now investigate the free energy of the above minimal model satisfying $M_{-}^{(1)}(\mathbf{k}) \neq 0 \cap M_{-}^{(2)}(\mathbf{k}) \neq 0$. By differentiating Eq. (8) with respect to Δ_j and Δ_j^* $(j = 1, 2)$, the Ginzburg-Landau free energy for superconductivity is derived as follows (see Supplementary Note 2):

$$\begin{aligned}\mathcal{F} = {} & \alpha_1|\Delta_1|^2 + \alpha_2|\Delta_2|^2 + \beta_1|\Delta_1|^4 + \beta_2|\Delta_2|^4 \\ & + 4\tilde{\beta}|\Delta_1|^2|\Delta_2|^2 - \tilde{\beta}(\Delta_1^2\Delta_2^{*2} + \Delta_2^2\Delta_1^{*2}) \\ & + \sum_{\nu=x,y,z}(\kappa_{1,\nu}|\Delta_1|^2 + \kappa_{2,\nu}|\Delta_2|^2)q_\nu^2 + \mathbf{T} \cdot \mathbf{q},\end{aligned} \tag{9}$$

where $\mathbf{q} = (q_x, q_y, q_z)$ is the center-of-mass momentum of Cooper pairs. The analytical expressions of α_j, $\beta_j(>0)$, $\tilde{\beta}(>0)$, and $\kappa_{j,\nu}(>0)$ are shown in Supplementary Note 2. The last term is the Lifshitz invariant[43] stabilizing the FFLO state with $\mathbf{q} \| \mathbf{T}$. Since the Cooper pair condensation occurs at a single $\mathbf{q}$ in our model, the superconducting order parameter is expressed as $\Delta(\mathbf{r}) \propto e^{i\mathbf{q}\cdot\mathbf{r}}$ in real space (Fig. 1c). The coefficient vector $\mathbf{T} = (T_x, T_y, T_z)$ is given by

$$\mathbf{T} = \rho_0\langle \mathrm{Tr}[M_{-}^{(1)}(\mathbf{k})\tilde{H}_0(\mathbf{k})]\mathbf{v}_{\mathbf{k}}\rangle_{\mathrm{FS}}\frac{7\zeta(3)}{16\pi^2T^2}, \tag{10}$$

where ρ_0 is the density of states at the Fermi energy, $\langle \cdots \rangle_{\mathrm{FS}}$ denotes the average over the Fermi surface, $\mathbf{v}_{\mathbf{k}} \equiv \nabla_{\mathbf{k}}\xi_{\mathbf{k}}$, T is the temperature, and $\zeta(x)$ is the Riemann zeta function. $\mathbf{T}$ can be interpreted as the effective anapole moment of the superconducting state. To see this, we here consider conditions for $\mathbf{T} \neq \mathbf{0}$. Eq. (10) indicates that $\mathbf{T}$ is nonzero only for $\mathcal{P}$- and $\mathcal{T}$-symmetry breaking pairing states with $M_{-}^{(1)}(\mathbf{k}) \neq 0$. In addition, $\langle \mathrm{Tr}[M_{-}^{(1)}(\mathbf{k})\tilde{H}_0(\mathbf{k})]\mathbf{v}_{\mathbf{k}}\rangle_{\mathrm{FS}}$ is nonzero only when the superconducting order parameter belongs to a polar irreducible representation (IR), since the velocity $\mathbf{v}_{\mathbf{k}}$ is a polar vector and $\tilde{H}_0(\mathbf{k})$ is assumed to be $\mathcal{P}$-symmetric. Therefore, $\mathbf{T}$ is a polar and time-reversal-odd vector; the symmetry is equivalent to the anapole moment[44,45]. Hereafter, we refer to the superconductivity with $\mathbf{T} \neq \mathbf{0}$ as the anapole superconductivity. The anapole superconductivity realizes a nonuniform FFLO state with $\mathbf{q} \| \mathbf{T}$ (see Fig. 1c) to compensate a polar asymmetry in the BS. The $\mathcal{PT}$-symmetric mixed-parity pairing is an origin of the anapole

superconductivity. Although the stability of such pairing has been revealed[15], a self-consistent calculation is desirable to justify the stability of the anapole FFLO state and clarify the properties further. Such detailed analysis is left for future work.

Finally, we comment that the anapole moment must be aligned in the conducting direction in low-dimensional systems. This restriction naturally appears through the above expression (10) of the effective anapole moment **T**.

Application to UTe_2. We now discuss the asymmetric BS and anapole superconductivity in UTe_2. Intensive studies after the discovery of superconductivity evidenced odd-parity spin-triplet superconductivity in UTe_2[54–56,66–79]. However, multiple superconducting phases similar to Fig. 1a have been observed under pressure[26–33], and the antiferromagnetic quantum criticality implies the spin-singlet superconductivity there[31]. A theoretical study based on the periodic Anderson model verified this naive expectation and predicted the parity-mixed superconducting state in the intermediate pressure region[25]. Note that the interband pairing, which is an essential ingredient for the asymmetric BS and anapole superconductivity, may have considerable impacts on the superconductivity in UTe_2 owing to multiple bands near the Fermi level[25,80–86].

First, let us discuss the symmetry of superconductivity. Since the crystal structure of UTe_2 preserves D_{2h} point group symmetry, the superconducting order parameter is classified based on the IRs of D_{2h}. Below we consider all the odd-parity IRs, namely, A_u, B_{1u}, B_{2u}, and B_{3u}, although the A_u and B_{3u} IRs may be promising candidates[25,77,78,80,87]. Moreover, a recent calculation has shown that the even-parity A_g superconducting state is favored by antiferromagnetic fluctuation under pressure[25]. Therefore, we study a mixture of the even-parity A_g and odd-parity either A_u, B_{1u}, B_{2u}, or B_{3u} states, while we particularly focus on the A_u or B_{3u} pairing.

Based on the above facts, we introduce a minimal model for UTe_2 as follows:

$$H_0(\mathbf{k}) = (\varepsilon_{\mathbf{k}} - \mu)\sigma_0 \otimes \tau_0 + \mathbf{g}_{\mathbf{k}} \cdot \boldsymbol{\sigma} \otimes \tau_z, \tag{11}$$

$$\hat{\Delta}(\mathbf{k}) = \Delta_1(\psi^{\mathrm{g}}_{\mathbf{k}}\sigma_0 \otimes \tau_0 + \mathbf{d}^{\mathrm{g}}_{\mathbf{k}} \cdot \boldsymbol{\sigma} \otimes \tau_z) + \Delta_2(\mathbf{d}^{\mathrm{u}}_{\mathbf{k}} \cdot \boldsymbol{\sigma} \otimes \tau_0 + \psi^{\mathrm{u}}_{\mathbf{k}}\sigma_0 \otimes \tau_z), \tag{12}$$

where τ_ν represent the Pauli matrices for a sublattice DOF originating from a ladder structure of U atoms (Fig. 2). We assume a simple form of the single-particle kinetic energy as $\varepsilon_{\mathbf{k}} = -2\sum_{\nu=x,y,z} t_\nu \cos k_\nu$. The second term of Eq. (11) is a sublattice-dependent staggered form of Rashba SOC with $\mathbf{g}_{\mathbf{k}} = \alpha(\sin k_y \hat{\mathbf{x}} - \sin k_x \hat{\mathbf{y}})$, arising from the local $\mathcal{P}$-symmetry breaking at U sites[25,88]. Since the local site symmetry descends to C_{2v} from D_{2h} owing to the ladder structure of U atoms, the existence of the Rashba-type SOC with opposite coupling constants $\pm\alpha$ at each sublattice is naturally expected (see Fig. 2). The local $\mathcal{P}$-symmetry breaking also leads to a sublattice-dependent parity mixing of the pair potential[89]. Then, the even-parity (odd-parity) pair potential is assumed to be a mixture of intrasublattice spin-singlet (spin-triplet) and staggered spin-triplet (spin-singlet) components as shown in Eq. (12). We assume the form of the **k**-dependent coefficients $\psi^{\mathrm{g}}_{\mathbf{k}}$ and $\mathbf{d}^{\mathrm{g}}_{\mathbf{k}}$ ($\mathbf{d}^{\mathrm{u}}_{\mathbf{k}}$ and $\psi^{\mathrm{u}}_{\mathbf{k}}$) so as to be consistent with the basis functions of the A_g IR (A_u, B_{1u}, B_{2u}, or B_{3u} IRs).

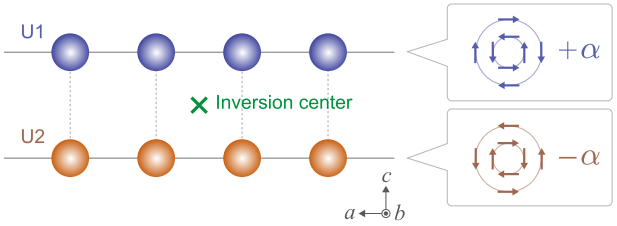

Fig. 2 Schematic of local $\mathcal{P}$-symmetry breaking in UTe_2. U atoms form a ladder structure along the a axis. The ladder structure generates two non-equivalent sublattices U1 (blue circle) and U2 (orange circle). Since the $\mathcal{P}$-symmetry is locally broken in this crystal structure, a sublattice-dependent Rashba-type spin-orbit coupling (SOC) appears. To maintain the global $\mathcal{P}$-symmetry, the magnitude of Rashba SOC α changes sign at each sublattice (i.e., $+\alpha$ for U1 and $-\alpha$ for U2).

We now consider the necessary conditions for an asymmetric BS in UTe_2. As discussed in the above sections, a nonzero $\mathrm{Tr}[M^{(1)}_{-}(\mathbf{k})\tilde{H}_0(\mathbf{k})]$ is necessary for the asymmetric BS in a two-band model. For Eqs. (11) and (12), this quantity is obtained as $\mathrm{Tr}[M^{(1)}_{-}(\mathbf{k})\tilde{H}_0(\mathbf{k})] = -8\mathrm{Im}(\Delta_1\Delta_2^*)[\mathbf{g}_{\mathbf{k}} \cdot (\mathbf{d}^{\mathrm{g}}_{\mathbf{k}} \times \mathbf{d}^{\mathrm{u}}_{\mathbf{k}})]$. Therefore, $\mathbf{g}_{\mathbf{k}} \cdot (\mathbf{d}^{\mathrm{g}}_{\mathbf{k}} \times \mathbf{d}^{\mathrm{u}}_{\mathbf{k}}) \neq 0$ must be satisfied to realize the asymmetric BS. This indicates that the sublattice-dependent SOC and spin-triplet pairing components $\mathbf{d}^{\mathrm{g,u}}_{\mathbf{k}}$ are essential for the asymmetric BS. In contrast, the spin-singlet pairing components $\psi^{\mathrm{g,u}}_{\mathbf{k}}$ do not play an important role for realizing the asymmetric BS in this model. Hereafter, we assume $\psi^{\mathrm{g}}_{\mathbf{k}} = 1$ and $\psi^{\mathrm{u}}_{\mathbf{k}} = 0$ for simplicity. The basis functions of $\mathbf{d}^{\mathrm{g,u}}_{\mathbf{k}}$ and corresponding $\mathbf{g}_{\mathbf{k}} \cdot (\mathbf{d}^{\mathrm{g}}_{\mathbf{k}} \times \mathbf{d}^{\mathrm{u}}_{\mathbf{k}})$ for possible mixed-parity superconducting states in UTe_2 are summarized in Table 1. As shown in Table 1, $\mathbf{g}_{\mathbf{k}} \cdot (\mathbf{d}^{\mathrm{g}}_{\mathbf{k}} \times \mathbf{d}^{\mathrm{u}}_{\mathbf{k}}) \propto \alpha(\phi^{\mathrm{g}}_x + \phi^{\mathrm{g}}_y)\phi^{\mathrm{u}}_z$ for all patterns of the superconducting state, where $\phi^{\mathrm{g,u}}_\nu$ is a real-valued coefficient of the ν-th component of $\mathbf{d}^{\mathrm{g,u}}_{\mathbf{k}}$. Therefore, $\phi^{\mathrm{g}}_x + \phi^{\mathrm{g}}_y \neq 0$ and $\phi^{\mathrm{u}}_z \neq 0$ are necessary for the asymmetric BS. According to a recent numerical calculation[25], the magnetic anisotropy of UTe_2 leads to $|\phi^{\mathrm{g}}_y| \gg |\phi^{\mathrm{g}}_x|$ for the A_g state. Then, we assume $\mathbf{d}^{\mathrm{g}}_{\mathbf{k}} = \sin k_x \hat{\mathbf{y}}$ (i.e., $\phi^{\mathrm{g}}_x = 0$ and $\phi^{\mathrm{g}}_y = 1$) in the following calculations. On the other hand, we assume $\phi^{\mathrm{u}}_\nu = \delta_{\nu z}$ for the odd-parity pairing component to extract only the essential ingredient for the asymmetric BS and make a clear discussion.

The numerical results of the BS for this UTe_2 model are shown in Fig. 3. We here consider only the $A_g + iA_u$ ($\mathbf{d}^{\mathrm{u}}_{\mathbf{k}} = \sin k_z \hat{\mathbf{z}}$) and $A_g + iB_{3u}$ ($\mathbf{d}^{\mathrm{u}}_{\mathbf{k}} = \sin k_y \hat{\mathbf{z}}$) states as promising candidates of the $\mathcal{PT}$-symmetric mixed-parity superconductivity in UTe_2. It is shown that the BS of both $A_g + iA_u$ and $A_g + iB_{3u}$ states are indeed asymmetric along some directions in the Brillouin zone (see Fig. 3a, b). The BS in the $A_g + iA_u$ state exhibits a $k_xk_yk_z$-type tetrahedral asymmetry as depicted in Fig. 3c, while the BS in the $A_g + iB_{3u}$ state shows a $k_xk_y^2$-type unidirectional asymmetry as depicted in Fig. 3d. Consistent with these numerical results, Table 1 reveals that $\mathbf{g}_{\mathbf{k}} \cdot (\mathbf{d}^{\mathrm{g}}_{\mathbf{k}} \times \mathbf{d}^{\mathrm{u}}_{\mathbf{k}})$ of the $A_g + iA_u$ and $A_g + iB_{3u}$ states are proportional to $k_xk_yk_z$ and $k_xk_y^2$, respectively. This implies that the type of asymmetry in the BS is determined by the symmetry of $\mathrm{Tr}[M^{(1)}_{-}(\mathbf{k})\tilde{H}_0(\mathbf{k})]$, which is an essential ingredient for realizing the asymmetric BS.

Finally, we discuss the possible anapole superconductivity in UTe_2. The $A_g + iA_u$ state belongs to the nonpolar A_u^- IR (IRs with odd time-reversal parity are denoted by Γ^-), which corresponds to nonpolar odd-parity magnetic multipoles such as magnetic monopole, quadrupole, and hexadecapole from the viewpoint of symmetry. On the other hand, the $A_g + iB_{3u}$ state belongs to the polar B_{3u}^- IR with the polar x axis, which is symmetrically equivalent to the anapole moment T_x. Since the anapole superconducting states are allowed only when the superconducting order parameter belongs to a polar IR, the $A_g + iB_{3u}$ state is a possible candidate of the anapole superconductivity. Indeed, as discussed above, the BS of the $A_g + iB_{3u}$ state exhibits a polar $k_xk_y^2$-type asymmetry, while the BS of the $A_g + iA_u$ state exhibits a

Table 1 Symmetry analysis of Bogoliubov spectrum asymmetry for UTe_2.

Pairing	$\mathbf{d}^{g}_{\mathbf{k}}$	$\mathbf{d}^{u}_{\mathbf{k}}$	$\mathbf{g}_{\mathbf{k}} \cdot (\mathbf{d}^{g}_{\mathbf{k}} \times \mathbf{d}^{u}_{\mathbf{k}})$	$\mathbf{T}$
$A_g + iA_u$	$\phi^g_x k_y \hat{\mathbf{x}} + \phi^g_y k_x \hat{\mathbf{y}}$	$\phi^u_x k_x \hat{\mathbf{x}} + \phi^u_y k_y \hat{\mathbf{y}} + \phi^u_z k_z \hat{\mathbf{z}}$	$\alpha(\phi^g_x + \phi^g_y)\phi^u_z k_x k_y k_z$	$\mathbf{T} = \mathbf{0}$
$A_g + iB_{3u}$	$\phi^g_x k_y \hat{\mathbf{x}} + \phi^g_y k_x \hat{\mathbf{y}}$	$\phi^u_y k_z \hat{\mathbf{y}} + \phi^u_z k_y \hat{\mathbf{z}}$	$\alpha(\phi^g_x + \phi^g_y)\phi^u_z k_x k_y^2$	$\mathbf{T} \parallel \hat{\mathbf{x}}$
$A_g + iB_{2u}$	$\phi^g_x k_y \hat{\mathbf{x}} + \phi^g_y k_x \hat{\mathbf{y}}$	$\phi^u_x k_z \hat{\mathbf{x}} + \phi^u_z k_x \hat{\mathbf{z}}$	$\alpha(\phi^g_x + \phi^g_y)\phi^u_z k_x^2 k_y$	$\mathbf{T} \parallel \hat{\mathbf{y}}$
$A_g + iB_{1u}$	$\phi^g_x k_y \hat{\mathbf{x}} + \phi^g_y k_x \hat{\mathbf{y}}$	$\phi^u_x k_y \hat{\mathbf{x}} + \phi^u_y k_x \hat{\mathbf{y}} + \phi^u_z k_x k_y k_z \hat{\mathbf{z}}$	$\alpha(\phi^g_x + \phi^g_y)\phi^u_z k_x^2 k_y^2 k_z$	$\mathbf{T} \parallel \hat{\mathbf{z}}$

Basis functions of $\mathbf{d}^{g,u}_{\mathbf{k}}$ and corresponding $\mathbf{g}_{\mathbf{k}} \cdot (\mathbf{d}^{g}_{\mathbf{k}} \times \mathbf{d}^{u}_{\mathbf{k}})$ for possible $\mathcal{PT}$-symmetric mixed-parity pairing states in UTe_2 are shown. The last column shows the form of the effective anapole moment $\mathbf{T}$ for each pairing state.

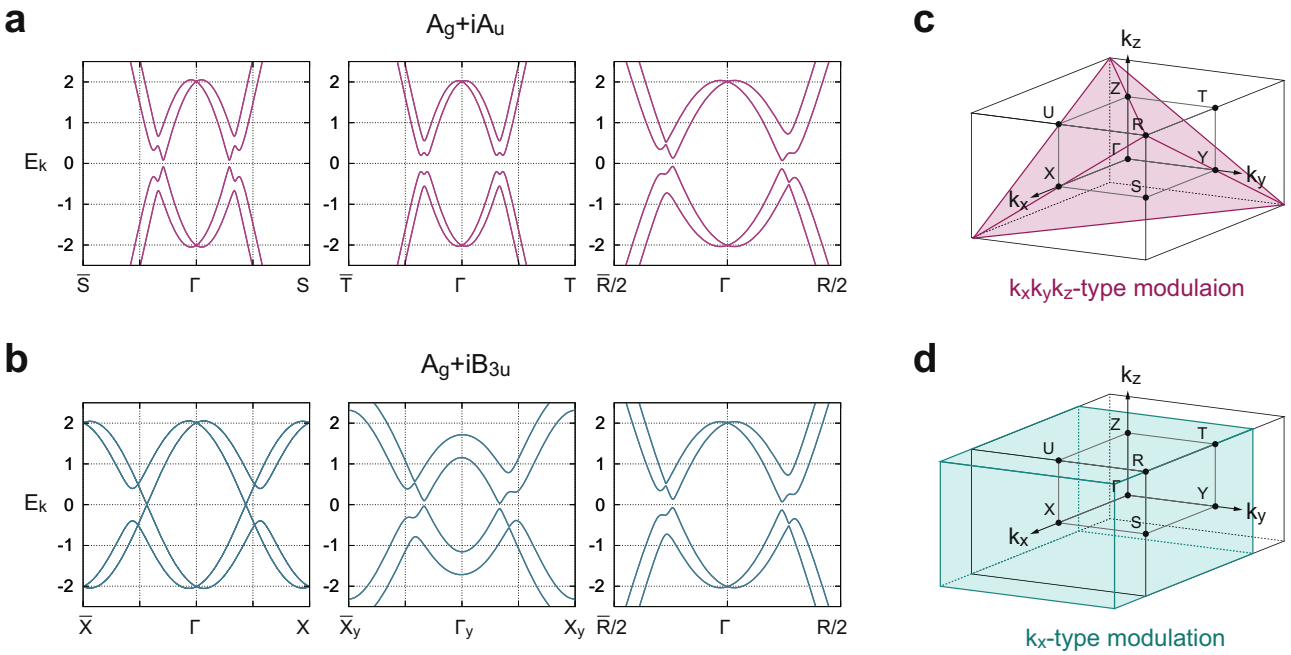

Fig. 3 Asymmetric Bogoliubov spectrum (BS) for the UTe_2 model. a, **b** Numerical results of BS in the UTe_2 model for the $A_g + iA_u$ state and the $A_g + iB_{3u}$ state. **c** Schematic of $k_xk_yk_z$-type asymmetric modulation in the Brillouin zone that is induced in the BS of $A_g + iA_u$ state in **a**. **d** Schematic of k_x-type asymmetric modulation that is induced in the BS of $A_g + iB_{3u}$ state in **b**. The symbols of the horizontal axis in **a** and **b** denote the **k**-points in the Brillouin zone of a primitive orthorhombic lattice; $\Gamma = (0, 0, 0)$, $X = -\bar{X} = (\pi, 0, 0)$, $S = -\bar{S} = (\pi, \pi, 0)$, $T = -\bar{T} = (0, \pi, \pi)$, $R = -\bar{R} = (\pi, \pi, \pi)$, $\Gamma_y = (0, \pi/4, 0)$, and $X_y = -\bar{X}_y = (\pi, \pi/4, 0)$. In the numerical calculations, parameters are set to be $t_\nu = 1.0$, $\mu = -4.0$, $\alpha = 0.4$, and $(\Delta_1, \Delta_2) = (0.2, 0.2i)$. The BS asymmetry appears in **a** and **b** consistent with the symmetry analysis of $\mathrm{Tr}[M^{(1)}_{-}(\mathbf{k})\tilde{H}_0(\mathbf{k})] \propto \mathbf{g}_{\mathbf{k}} \cdot (\mathbf{d}^{g}_{\mathbf{k}} \times \mathbf{d}^{u}_{\mathbf{k}})$.

nonpolar $k_xk_yk_z$-type asymmetry (see Fig. 3). It should also be noted that the BS in the $A_g + iB_{3u}$ state possesses the polarity along the k_x axis, which coincides with the polar axis of the B^-_{3u} IR.

Based on the above classification and the Ginzburg-Landau free energy (9), the anapole FFLO state with $\mathbf{q} \propto \mathbf{T} \parallel \hat{\mathbf{x}}$ should be naturally realized in the $A_g + iB_{3u}$ state. In the same manner, we expect the anapole superconducting states with $\mathbf{T} \parallel \hat{\mathbf{y}}$ and $\mathbf{T} \parallel \hat{\mathbf{z}}$ in the $A_g + iB_{2u}$ and $A_g + iB_{1u}$ states, respectively (see Supplementary Note 3 for possible anapole superconductivity in UTe_2).

Discussion

From the analogy with magnetic states, we can predict various exotic superconducting phenomena closely related to the asymmetric BS. For instance, the asymmetry of the BS will significantly affect the superconducting piezoelectric effect[90], nonreciprocal optical responses[91], and nonreciprocal Meissner effect[92]. All of these phenomena are caused by the absence of $\mathcal{P}$- and $\mathcal{T}$-symmetries in the superconducting state. Hence, they will be useful probes to offer conclusive evidence for the $\mathcal{P}, \mathcal{T}$-symmetry breaking and the BS asymmetry in superconductors. Studies for the interplay of these exotic superconducting phenomena and asymmetric BS will be presented elsewhere.

Experimental detection of the anapole superconductivity should be possible by observing its domain structure. The anapole superconducting state effectively carries a supercurrent along the anapole moment $\mathbf{T}$, since the order parameter is spatially modulated with $e^{i\mathbf{q}\cdot\mathbf{r}} \sim e^{i\mathbf{T}\cdot\mathbf{r}}$. This indicates the emergence of superconducting vortices at the anapole domain boundaries (see Fig. 4a) even though an external magnetic field is absent. The anapole domains can be generally formed owing to the degeneracy between the $\Gamma_g + i\Gamma_u$ pairing and $\Gamma_g - i\Gamma_u$ pairing states, which have the opposite anapole moment. Therefore, the observation of vortices at a zero magnetic field can be solid evidence of the anapole superconductivity. In addition, the anapole domain can be switched by the supercurrent in a similar way to the electrical switching of antiferromagnets[93,94]. In an anapole superconductor, the effective anapole moment $\mathbf{T}$ couples to the applied electric current $\mathbf{j}$, which is a symmetry-adapted field of the anapole moment. Then, the anapole superconducting domain

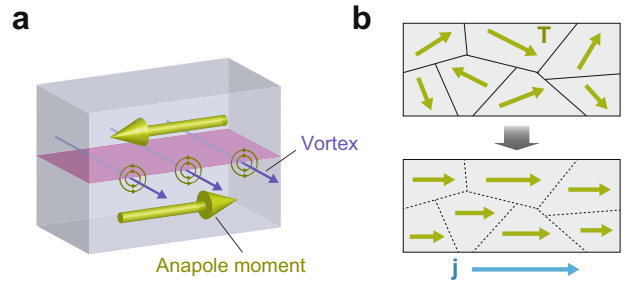

Fig. 4 Anapole domain and domain switching through supercurrent. a Vortices at the boundary of anapole superconducting domains. **b** The proposed domain switching in anapole superconductors. The effective anapole moment **T** is aligned along the injected supercurrent **j**.

should be switched to align the effective anapole moments along the injected supercurrent **j** (see Fig. 4b). It should also be noticed that the anapole domain switching eliminates the internal magnetic field from the vortices at the domain boundaries, since the domain structure disappears by applying the supercurrent. Therefore, the anapole superconducting domain switching can be regarded as a process of erasing magnetic information. These properties indicate potential applications of anapole superconductivity as a novel quantum device for magnetic information storage and processing.

Conclusions

In summary, we have established that the $\mathcal{PT}$-symmetric mixed-parity superconductors generally exhibit asymmetry in the BS. The essential ingredient for the asymmetric BS is the $\mathcal{P},\mathcal{T}$-odd nonunitary part of the bilinear product $\Delta\Delta^\dagger$ arising from the interband pairing. Therefore, the multiband nature of superconductivity is essential. Especially, we have shown that an FFLO state is stabilized in the absence of an external magnetic field when the superconducting state belongs to a polar and time-reversal-odd IR. The stabilization of the FFLO state is evidenced by the emergence of Lifshitz invariants in the free energy due to the effective anapole moment. The physics of asymmetric BS appears in any multiband superconductors when even- and odd-parity pairing interactions are comparable in strength. As a specific example, we considered the mixed-parity pairing states in UTe_2, which is caused by an accidental competition of ferromagnetic and antiferromagnetic spin fluctuations under pressure[25]. We have shown that the mixed-parity superconductivity in UTe_2 realizes the asymmetric BS and anapole superconductivity owing to the locally noncentrosymmetric crystal structure. The asymmetric BS may be linked to the asymmetric spectrum in the scanning tunneling microscope measurement[55], although it was interpreted based on the chiral superconductivity. The vortex structure near the anapole domain boundary (Fig. 4a) may also cause the polar Kerr effect, reported for UTe_2[58]. Spontaneous ordering of strongly parity-mixed pairing state and resulting asymmetric BS can also be expected in superconductivity mediated by parity-breaking fluctuations[11]. To further broaden the scope of application of our theory, it is important to find microscopic electronic interactions that induce competing even- and odd-parity pairing instabilities.

We predicted various superconducting phenomena induced by the asymmetric BS, such as the superconducting piezoelectric effect, nonlinear optical responses, nonreciprocal Meissner effect, and anapole domain switching from the analogy with magnetic materials. Topological properties and collective modes associated with the asymmetric BS may also be intriguing issues. Exploration of such exotic phenomena will be a promising route for future research.

Table 2 Classification of two-band models based on the extra degrees of freedom (DOF).

	(x_i, y_i, z_i)	U_P	U_T	DOF
$i=1$	(x, y, z)	$\sigma_0 \otimes \tau_0$	$i\sigma_y \otimes \tau_0$	orbitals (same parity)
$i=2$	(z, x, y)	$\sigma_0 \otimes \tau_z$	$i\sigma_y \otimes \tau_0$	orbitals (opposite parity)
$i=3$	(y, z, x)	$\sigma_0 \otimes \tau_x$	$i\sigma_y \otimes \tau_0$	sublattices

Definition of (x_i, y_i, z_i), U_P, U_T, and physical meaning of the extra DOF for $i=1, 2, 3$ are listed. Here, U_P and U_T are unitary matrices representing the parity and time-reversal operations. σ_μ and τ_μ ($\mu=0, x, y, z$) are the Pauli matrices for the spin and extra DOF.

Methods

Correspondence between Pauli matrices and Dirac matrices. In this section, we show that the general form of the BdG Hamiltonian with spin-1/2 and a two-valued extra DOF can be expressed by using the Euclidean Dirac matrices.

Since we assume that the normal state preserves both $\mathcal{P}$- and $\mathcal{T}$-symmetries, $H_0(\mathbf{k})$ transforms under the space-inversion $\mathcal{P}$ and the time-reversal $\mathcal{T}$ as

$$H_0(\mathbf{k}) \xrightarrow{\mathcal{P}} U_P^\dagger H_0(-\mathbf{k}) U_P = H_0(\mathbf{k}), \tag{13}$$

$$H_0(\mathbf{k}) \xrightarrow{\mathcal{T}} U_T^\dagger H_0^*(-\mathbf{k}) U_T = H_0(\mathbf{k}), \tag{14}$$

where U_P and U_T are unitary matrices. In this paper, we consider a spin-1/2 system satisfying $U_T U_T^* = -\mathbf{1}_4$. In addition, we require that the time-reversal commute with the space-inversion (i.e., $U_P U_T = U_T U_P^*$), and the space-inversion operator is its own inverse (i.e., $U_P^2 = \mathbf{1}_4$). Under the above assumptions, $H_0(\mathbf{k})$ can be generally expressed as

$$\begin{aligned} H_0(\mathbf{k}) = (\epsilon_{\mathbf{k}}^0 - \mu)\sigma_0 \otimes \tau_0 + f_{\mathbf{k}}\sigma_0 \otimes \tau_{x_i} \\ + \mathbf{g}_{\mathbf{k}} \cdot \boldsymbol{\sigma} \otimes \tau_{y_i} + h_{\mathbf{k}}\sigma_0 \otimes \tau_{z_i}, \end{aligned} \tag{15}$$

where $\boldsymbol{\sigma} = (\sigma_x, \sigma_y, \sigma_z)$ and $\sigma_0 \otimes \tau_0 = \mathbf{1}_4$. Hermiticity requires all coefficients in Eq (15) are real. The index i specifies the extra DOF and (x_i, y_i, z_i) is a permutation of (x, y, z). Since U_P and U_T vary depending on the extra DOF, the general models (15) are classified by the index i. In this paper, we consider three representative examples shown in Table 2. For $i=1$ ($i=2$), the extra DOF is orbitals with the same (opposite) parity, and $U_P = \sigma_0 \otimes \tau_0$ ($U_P = \sigma_0 \otimes \tau_z$). For $i=3$, the extra DOF is sublattices in a locally noncentrosymmetric crystal structure, and $U_P = \sigma_0 \otimes \tau_x$. In these cases, $U_T = i\sigma_y \otimes \tau_0$. Although the extra DOF can be other than the above three cases, Eq. (15) holds for all the cases unless $U_P U_T \neq U_T U_P^*$, $U_P U_P \neq \mathbf{1}_4$, or $U_T U_T^* \neq -\mathbf{1}_4$[37]. Since the set of $\sigma_\mu \otimes \tau_\nu$ matrices is completely anticommuting in Eq. (15), we can substitute them by the five anticommuting Euclidean Dirac matrices. Then, we can rewrite Eq. (15) as Eq. (2).

The pairing potential $\Delta(\mathbf{k})$ transforms under the space-inversion and the time-reversal as $\Delta(\mathbf{k}) \xrightarrow{\mathcal{P}} U_P^\dagger \Delta(-\mathbf{k}) U_P^*$ and $\Delta(\mathbf{k}) \xrightarrow{\mathcal{T}} U_T^\dagger \Delta^*(-\mathbf{k}) U_T^*$, respectively. In terms of $\hat{\Delta}(\mathbf{k}) = \Delta(\mathbf{k}) U_T^\dagger$, these relations can be rewritten as

$$\hat{\Delta}(\mathbf{k}) \xrightarrow{\mathcal{P}} U_P^\dagger \hat{\Delta}(-\mathbf{k}) U_P, \tag{16}$$

$$\hat{\Delta}(\mathbf{k}) \xrightarrow{\mathcal{T}} \hat{\Delta}^\dagger(\mathbf{k}). \tag{17}$$

We note that Eq. (16) is equivalent to the transformation of $H_0(\mathbf{k})$ under the space-inversion [see Eq. (13)], while Eq. (17) corresponds to the Hermiticity condition. Whereas $H_0(\mathbf{k})$ is assumed to preserve both $\mathcal{P}$- and $\mathcal{T}$-symmetries, we admit that $\Delta(\mathbf{k})$ spontaneously breaks the $\mathcal{P}$- and $\mathcal{T}$-symmetries. The only requirements for the pairing potential is satisfying the fermionic antisymmetry $\Delta(\mathbf{k}) = -\Delta^{\mathrm{T}}(-\mathbf{k})$, which can be rewritten as

$$\hat{\Delta}(\mathbf{k}) = U_T^\dagger \hat{\Delta}^{\mathrm{T}}(-\mathbf{k}) U_T, \tag{18}$$

where we used the fact that $U_T^\dagger = U_T^{\mathrm{T}} = -U_T$ by choosing U_T as real (i.e., $U_T = U_T^*$). It should be noticed that Eq. (18) is formally equivalent to the time-reversal symmetry for $H_0(\mathbf{k})$ [see Eq. (14)]. Since the even-parity part of $\hat{\Delta}(\mathbf{k})$ obeys transformation properties completely equivalent to those of $H_0(\mathbf{k})$ under the time-reversal and the space-inversion, it can be expressed as a linear combination of six $\sigma_\mu \otimes \tau_\nu$ matrices allowed to appear in $H_0(\mathbf{k})$. On the other hand, the other ten $\sigma_\mu \otimes \tau_\nu$ matrices, which correspond to $i\gamma_m\gamma_n$ ($1 \le m < n \le 5$), constitute the odd-parity pairing potential. Then, we obtain a general form of $\Delta(\mathbf{k})$ as

Table 3 Necessary conditions for the asymmetric Bogoliubov spectrum in two-band models ($\sigma_\mu \otimes \tau_\nu$ basis).

	Criterion (i)	Criterion (ii)
(I)		$\psi_{\mathbf{k}}^{z_i}\psi_{\mathbf{k}}^{y_i} f_{\mathbf{k}} \neq 0$
(II)		$(\mathbf{d}_{\mathbf{k}}^{y_i} \cdot \mathbf{d}_{\mathbf{k}}^{z_i}) f_{\mathbf{k}} \neq 0$
(III)		$\psi_{\mathbf{k}}^{x_i}(\mathbf{d}_{\mathbf{k}}^{z_i} \cdot \mathbf{g}_{\mathbf{k}}) \neq 0$
(IV)	$\mathrm{Im}(\Delta_1\Delta_2^*) \neq 0$	$\psi_{\mathbf{k}}^{z_i}(\mathbf{d}_{\mathbf{k}}^{x_i} \cdot \mathbf{g}_{\mathbf{k}}) \neq 0$
(V)		$(\mathbf{d}_{\mathbf{k}}^{y_i} \times \mathbf{d}_{\mathbf{k}}^{0}) \cdot \mathbf{g}_{\mathbf{k}} \neq 0$
(VI)		$(\mathbf{d}_{\mathbf{k}}^{y_i} \cdot \mathbf{d}_{\mathbf{k}}^{x_i}) h_{\mathbf{k}} \neq 0$
(VII)		$\psi_{\mathbf{k}}^{x_i}\psi_{\mathbf{k}}^{y_i} h_{\mathbf{k}} \neq 0$

If both criteria (i) and (ii) are satisfied, asymmetric Bogoliubov spectrum can be realized in two-band models.

$$\hat{\Delta}(\mathbf{k}) = \Delta_1\left[\sum_{\nu=0,x_i,z_i}\psi_{\mathbf{k}}^{\nu}\sigma_0\otimes\tau_\nu + \mathbf{d}_{\mathbf{k}}^{y_i}\cdot\boldsymbol{\sigma}\otimes\tau_{y_i}\right] + \Delta_2\left[\sum_{\nu=0,x_i,z_i}\mathbf{d}_{\mathbf{k}}^{\nu}\cdot\boldsymbol{\sigma}\otimes\tau_\nu + \psi_{\mathbf{k}}^{y_i}\sigma_0\otimes\tau_{y_i}\right], \tag{19}$$

where $\psi_{\mathbf{k}}^{\nu}$ and $\mathbf{d}_{\mathbf{k}}^{\nu}$ are real-valued coefficients. Note that Δ_1 and Δ_2 are complex valued since $\hat{\Delta}(\mathbf{k}) \neq \hat{\Delta}^\dagger(\mathbf{k})$ in $\mathcal{T}$-symmetry breaking superconducting phases. From Eq. (19), we obtain Eq. (3) as a general form of $\Delta(\mathbf{k})$ in two-band models.

From Eqs. (15) and (19), we obtain

$$\begin{aligned}\mathrm{Tr}[M_-^{(1)}(\mathbf{k})\check{H}_0(\mathbf{k})] = 8\mathrm{Im}(\Delta_1\Delta_2^*)\times\big[&(\psi_{\mathbf{k}}^{z_i}\psi_{\mathbf{k}}^{y_i} - \mathbf{d}_{\mathbf{k}}^{y_i}\cdot\mathbf{d}_{\mathbf{k}}^{z_i})f_{\mathbf{k}}\\ &+ (\psi_{\mathbf{k}}^{x_i}\mathbf{d}_{\mathbf{k}}^{z_i} - \psi_{\mathbf{k}}^{z_i}\mathbf{d}_{\mathbf{k}}^{x_i} - \mathbf{d}_{\mathbf{k}}^{y_i}\times\mathbf{d}_{\mathbf{k}}^{0})\cdot\mathbf{g}_{\mathbf{k}}\\ &+ (\mathbf{d}_{\mathbf{k}}^{y_i}\cdot\mathbf{d}_{\mathbf{k}}^{x_i} - \psi_{\mathbf{k}}^{x_i}\psi_{\mathbf{k}}^{y_i})h_{\mathbf{k}}\big].\end{aligned} \tag{20}$$

Then, in the $\sigma_\mu \otimes \tau_\nu$ basis, the necessary conditions for the asymmetric BS (i.e., $\mathrm{Tr}[M_-^{(1)}(\mathbf{k})\check{H}_0(\mathbf{k})] \neq 0$) can be summarized as shown in Table 3. For example, the condition (I) means that the asymmetric BS appears when $\mathrm{Im}(\Delta_1\Delta_2^*) \neq 0$ and $\psi_{\mathbf{k}}^{z_i}\psi_{\mathbf{k}}^{y_i} f_{\mathbf{k}} \neq 0$.

Asymmetry of BS in the minimal two-band model. We here prove that Eq. (8) indeed expresses the asymmetric BS. For $r = 1$, Eq. (8) leads to

$$E_{\mathbf{k}}^{\pm} = \sqrt{\xi_{\mathbf{k}}^2 + |\Delta_1\eta_{\mathbf{k}}^b|^2 + |\Delta_2\eta_{\mathbf{k}}^{ab}|^2 \pm 2\mathrm{Im}(\Delta_1\Delta_2^*)\eta_{\mathbf{k}}^b\eta_{\mathbf{k}}^{ab}} \pm \epsilon_{\mathbf{k}}^a. \tag{21}$$

Then, we need to specify the $\mathbf{k}$-parity of $\epsilon_{\mathbf{k}}^a$, $\eta_{\mathbf{k}}^b$, and $\eta_{\mathbf{k}}^{ab}$, which depend on the details of the extra DOF, to investigate the property of the BS $E_{-\mathbf{k}}^{\pm}$. We here denote $\epsilon_{-\mathbf{k}}^a = p_a\epsilon_{\mathbf{k}}^a$, $\eta_{-\mathbf{k}}^b = p_b\eta_{\mathbf{k}}^b$, and $\eta_{-\mathbf{k}}^{ab} = p_{ab}\eta_{\mathbf{k}}^{ab}$ ($p_a, p_b, p_{ab} = \pm 1$). From Eqs. (13) and (14), we obtain $p_a\gamma_a = U_{\mathrm{T}}^\dagger\gamma_a^* U_{\mathrm{T}} = U_{\mathrm{P}}^\dagger\gamma_a U_{\mathrm{P}}$. On the other hand, the $\mathcal{P},\mathcal{T}$-odd behavior of $M^{(1)}(\mathbf{k}) = 2\mathrm{Im}(\Delta_1\Delta_2^*)\eta_{\mathbf{k}}^b\eta_{\mathbf{k}}^{ab}\gamma_a$ leads to $-p_bp_{ab}\gamma_a = U_{\mathrm{T}}^\dagger\gamma_a^* U_{\mathrm{T}} = U_{\mathrm{P}}^\dagger\gamma_a U_{\mathrm{P}}$. Thus, $p_a = -p_bp_{ab}$ holds in general. Using this relation, we obtain

$$E_{-\mathbf{k}}^{\pm} = \sqrt{\xi_{\mathbf{k}}^2 + |\Delta_1\eta_{\mathbf{k}}^b|^2 + |\Delta_2\eta_{\mathbf{k}}^{ab}|^2 \mp p_a 2\mathrm{Im}(\Delta_1\Delta_2^*)\eta_{\mathbf{k}}^b\eta_{\mathbf{k}}^{ab}} \pm p_a\epsilon_{\mathbf{k}}^a, \tag{22}$$

where $p_a = \pm 1$. Comparing Eq. (22) with (21), we can safely say that $E_{-\mathbf{k}}^{\pm} \neq E_{\mathbf{k}}^{+}, E_{\mathbf{k}}^{-}$ and the BS is asymmetric. In the same manner, we can prove the asymmetry of Eq. (8) for $r = 0$.

Data availability

The data that support the findings of this study are available from the corresponding author upon reasonable request.

Code availability

The codes used for the numerical calculations in this study are available from the corresponding author upon reasonable request.

Received: 14 July 2021; Accepted: 22 December 2021;
Published online: 10 February 2022

References

1. Sigrist, M. & Ueda, K. Phenomenological theory of unconventional superconductivity. *Rev. Mod. Phys.* **63**, 239–311 (1991).
2. Leggett, A. J. A theoretical description of the new phases of liquid ^{3}He. *Rev. Mod. Phys.* **47**, 331–414 (1975).
3. Hasan, M. Z. & Kane, C. L. Colloquium: Topological insulators. *Rev. Mod. Phys.* **82**, 3045–3067 (2010).
4. Qi, Xiao-g & Zhang, Shou-Cheng Topological insulators and superconductors. *Rev. Mod. Phys.* **83**, 1057–1110 (2011).
5. Taylor, E. & Kallin, C. Intrinsic hall effect in a multiband chiral superconductor in the absence of an external magnetic field. *Phys. Rev. Lett.* **108**, 157001 (2012).
6. Bauer, E. & Sigrist, M. eds., *Noncentrosymmetric Superconductor: Introduction and Overview* (Springer, Berlin, 2012).
7. Smidman, M., Salamon, M. B., Yuan, H. Q. & Agterberg, D. F. Superconductivity and spin–orbit coupling in non-centrosymmetric materials: a review. *Rep. Prog. Phys.* **80**, 036501 (2017).
8. Wu, C. & Hirsch, J. E. Mixed triplet and singlet pairing in ultracold multicomponent fermion systems with dipolar interactions. *Phys. Rev. B* **81**, 020508(R) (2010).
9. Hong, Zhou, L., Yi, W. & Cui, X. L. Fermion superfluid with hybridized *s*- and *p*-wave pairings. *Sci. China Phys. Mech. Astron.* **60**, 127011 (2017).
10. Fu, L. Parity-breaking phases of spin-orbit-coupled metals with gyrotropic, ferroelectric, and multipolar orders. *Phys. Rev. Lett.* **115**, 026401 (2015).
11. Kozii, V. & Fu, L. Odd-parity superconductivity in the vicinity of inversion symmetry breaking in spin-orbit-coupled systems. *Phys. Rev. Lett.* **115**, 207002 (2015).
12. Sumita, S. & Yanase, Y. Superconductivity induced by fluctuations of momentum-based multipoles. *Phys. Rev. Res.* **2**, 033225 (2020).
13. Hiroi, Z., Yamaura, J., Kobayashi, T. C., Matsubayashi, Y. & Hirai, D. Pyrochlore oxide superconductor $Cd_2Re_2O_7$ revisited. *J. Phys. Soc. Jpn.* **87**, 024702 (2018).
14. Schumann, T. et al. Possible signatures of mixed-parity superconductivity in doped polar $SrTiO_3$ films. *Phys. Rev. B* **101**, 100503(R) (2020).
15. Wang, Y. & Fu, L. Topological phase transitions in multicomponent superconductors. *Phys. Rev. Lett.* **119**, 187003 (2017).
16. Yang, W., Xu, C. & Wu, C. Single branch of chiral Majorana modes from doubly degenerate Fermi surfaces. *Phys. Rev. Res.* **2**, 042047(R) (2020).
17. Sergienko, I. A. Mixed-parity superconductivity in centrosymmetric crystals. *Phys. Rev. B* **69**, 174502 (2004).
18. Ryu, S., Moore, J. E. & Ludwig, A. W. W. Electromagnetic and gravitational responses and anomalies in topological insulators and superconductors. *Phys. Rev. B* **85**, 045104 (2012).
19. Qi, X.-g, Witten, E. & Zhang, S.-C. Axion topological field theory of topological superconductors. *Phys. Rev. B* **87**, 134519 (2013).
20. Goswami, P. & Roy, B. Axionic superconductivity in three-dimensional doped narrow-gap semiconductors. *Phys. Rev. B* **90**, 041301(R) (2014).
21. Shiozaki, K. & Fujimoto, S. Dynamical axion in topological superconductors and superfluids. *Phys. Rev. B* **89**, 054506 (2014).
22. Roy, B. H.-order topological superconductors in $\mathcal{P}$-, $\mathcal{P}$-odd quadrupolar Dirac materials. *Phys. Rev. B* **101**, 220506(R) (2020).
23. Xu, C. and Yang, W., Axion electrodynamics in *p+is* superconductors. https://arxiv.org/abs/2009.12998 (2020).
24. Scaffidi, T., Degeneracy between even-and odd-parity superconductivity in the quasi-1D Hubbard model and implications for Sr_2RuO_4. https://arxiv.org/abs/2007.13769 (2020).
25. Ishizuka, J. & Yanase, Y. Periodic Anderson model for magnetism and superconductivity in UTe_2. *Phys. Rev. B* **103**, 094504 (2021).
26. Braithwaite, D. et al. Multiple superconducting phases in a nearly ferromagnetic system. *Commun. Phys.* **2**, 1–6 (2019).
27. Ran, S. et al. Enhancement and reentrance of spin triplet superconductivity in UTe_2 under pressure. *Phys. Rev. B* **101**, 140503(R) (2020).
28. Lin, W. C. et al. Tuning magnetic confinement of spin-triplet superconductivity. *npj Quantum Mater.* **5**, 1–6 (2020).
29. Knebel, G. et al. Anisotropy of the upper critical field in the heavy-fermion superconductor UTe_2 under pressure. *J. Phys. Soc. Jpn.* **89**, 053707 (2020).
30. Aoki, D. et al. Multiple superconducting phases and unusual enhancement of the upper critical field in UTe_2. *J. Phys. Soc. Jpn.* **89**, 053705 (2020).
31. Thomas, S. M. et al. Evidence for a pressure-induced antiferromagnetic quantum critical point in intermediate-valence UTe2. *Sci. Adv.* **6**, eabc8709 (2020).
32. Thomas, S. M. et al. Spatially inhomogeneous superconductivity in UTe_2. *Phys. Rev. B* **104**, 224501 (2021).
33. Aoki, D. et al. Field-induced superconductivity near the superconducting critical pressure in UTe_2. *J. Phys. Soc. Jpn.* **90**, 074705 (2021).
34. Black-Schaffer, A. M. & Balatsky, A. V. Odd-frequency superconducting pairing in multiband superconductors. *Phys. Rev. B* **88**, 104514 (2013).
35. Wang, Z., Berlinsky, J., Zwicknagl, G. & Kallin, C. Intrinsic ac anomalous Hall effect of nonsymmorphic chiral superconductors with an application to UPt_3. *Phys. Rev. B* **96**, 174511 (2017).
36. Brydon, P. M. R., Abergel, D. S. L., Agterberg, D. F. & Yakovenko, V. M. Loop currents and anomalous hall effect from time-reversal symmetry-breaking superconductivity on the honeycomb lattice. *Phys. Rev. X* **9**, 031025 (2019).

37. Denys, M. D. E. & Brydon, P. M. R. Origin of the anomalous Hall effect in two-band chiral superconductors. *Phys. Rev. B* **103**, 094503 (2021).
38. Triola, C. & Black-Schaffer, A. M. Odd-frequency pairing and Kerr effect in the heavy-fermion superconductor UPt_3. *Phys. Rev. B* **97**, 064505 (2018).
39. Agterberg, D. F., Brydon, P. M. R. & Timm, C. Bogoliubov fermi surfaces in superconductors with broken time-reversal symmetry. *Phys. Rev. Lett.* **118**, 127001 (2017).
40. Brydon, P. M. R., Agterberg, D. F., Menke, H. & Timm, C. Bogoliubov Fermi surfaces: General theory, magnetic order, and topology. *Phys. Rev. B* **98**, 224509 (2018).
41. Fulde, P. & Ferrell, R. A. Superconductivity in a strong spin-exchange field. *Phys. Rev.* **135**, A550–A563 (1964).
42. Larkin, A. I. & Ovchinnikov, Y. N. Inhomogeneous state of superconductors. *Zh. Eksp. Teor. Fiz.* **47**, 1136 (1964). [translation: Sov. Phys. JETP 20, 762 (1965)].
43. Mineev, V. P. & Samokhin, K. V. Nonuniform states in noncentrosymmetric superconductors: Derivation of Lifshitz invariants from microscopic theory. *Phys. Rev. B* **78**, 144503 (2008).
44. Spaldin, N. A., Fiebig, M. & Mostovoy, M. The toroidal moment in condensed-matter physics and its relation to the magnetoelectric effect. *J. Phys.: Condens. Matter* **20**, 434203 (2008).
45. Flambaum, V. V., Khriplovich, I. B. & Sushkov, O. P. Nuclear anapole moments. *Phys. Lett. B* **146**, 367–369 (1984).
46. Jeong, J., Sidis, Y., Louat, A., Brouet, V. & Bourges, P. Time-reversal symmetry breaking hidden order in $Sr_2(Ir,Rh)O_4$. *Nat. Commun.* **8**, 15119 (2017).
47. Murayama, H. et al. Bond directional anapole order in a spin-orbit coupled mott insulator $Sr_2(Ir_{1-x}Rh_x)O_4$. *Phys. Rev. X* **11**, 011021 (2021).
48. Watanabe, H. & Yanase, Y. Chiral photocurrent in parity-violating magnet and enhanced response in topological antiferromagnet. *Phys. Rev. X* **11**, 011001 (2021).
49. Ahn, J., Guo, G.-Y. & Nagaosa, N. Low-frequency divergence and quantum geometry of the bulk photovoltaic effect in topological semimetals. *Phys. Rev. X* **10**, 041041 (2020).
50. Agterberg, D. F. & Kaur, R. P. Magnetic-field-induced helical and stripe phases in Rashba superconductors. *Phys. Rev. B* **75**, 064511 (2007).
51. Sumita, S. & Yanase, Y. Superconductivity in magnetic multipole states. *Phys. Rev. B* **93**, 224507 (2016).
52. Sumita, S., Nomoto, T. & Yanase, Y. Multipole superconductivity in nonsymmorphic Sr_2IrO_4. *Phys. Rev. Lett.* **119**, 027001 (2017).
53. Timm, C., Brydon, P. M. R. & Agterberg, D. F. Distortional weak-coupling instability of Bogoliubov Fermi surfaces. *Phys. Rev. B* **103**, 024521 (2021).
54. Ran, S. et al. Nearly ferromagnetic spin-triplet superconductivity. *Science* **365**, 684–687 (2019).
55. Jiao, L. et al. Chiral superconductivity in heavy-fermion metal UTe_2. *Nature* **579**, 523–527 (2020).
56. Hayes, I. M. et al. Weyl superconductivity in UTe_2. https://arxiv.org/abs/2002.02539 (2020).
57. Ishihara, K. et al. Chiral superconductivity in UTe_2 probed by anisotropic low-energy excitations. https://arxiv.org/abs/2105.13721 (2021).
58. Hayes, I. M. et al. Multicomponent superconducting order parameter in UTe_2. *Science* **373**, 797–801 (2021).
59. Yanase, Y. Magneto-electric effect in three-dimensional coupled zigzag chains. *J. Phys. Soc. Jpn.* **83**, 014703 (2014).
60. Hayami, S., Kusunose, H. & Motome, Y. Toroidal order in metals without local inversion symmetry. *Phys. Rev. B* **90**, 024432 (2014).
61. A. Rikken, G. L. J., Fölling, J. & Wyder, P. Electrical magnetochiral anisotropy. *Phys. Rev. Lett.* **87**, 236602 (2001).
62. Watanabe, H. & Yanase, Y. Magnetic hexadecapole order and magnetopiezoelectric metal state in $\mathbf{Ba_{1-x}K_xMn_2As_2}$. *Phys. Rev. B* **96**, 064432 (2017).
63. Shiomi, Y. et al. Observation of a magnetopiezoelectric effect in the antiferromagnetic metal $EuMnBi_2$. *Phys. Rev. Lett.* **122**, 127207 (2019).
64. Ramires, A. & Sigrist, M. Identifying detrimental effects for multiorbital superconductivity: application to Sr_2RuO_4. *Phys. Rev. B* **94**, 104501 (2016).
65. Ramires, A., Agterberg, D. F. & Sigrist, M. Tailoring T_c by symmetry principles: The concept of superconducting fitness. *Phys. Rev. B* **98**, 024501 (2018).
66. Aoki, D. et al. Unconventional superconductivity in heavy fermion UTe_2. *J. Phys. Soc. Jpn.* **88**, 043702 (2019).
67. Tokunaga, Y. et al. ^{125}Te-NMR study on a single crystal of heavy fermion superconductor UTe_2. *J. Phys. Soc. Jpn.* **88**, 073701 (2019).
68. Sundar, S. et al. Coexistence of ferromagnetic fluctuations and superconductivity in the actinide superconductor UTe_2. *Phys. Rev. B* **100**, 140502(R) (2019).
69. Knebel, G. et al. Field-reentrant superconductivity close to a metamagnetic transition in the heavy-fermion superconductor UTe_2. *J. Phys. Soc. Jpn.* **88**, 063707 (2019).
70. Knafo, W. et al. Magnetic-field-induced phenomena in the paramagnetic superconductor UTe_2. *J. Phys. Soc. Jpn.* **88**, 063705 (2019).
71. Miyake, A. et al. Metamagnetic transition in heavy fermion superconductor UTe_2. *J. Phys. Soc. Jpn.* **88**, 063706 (2019).
72. Imajo, S. et al. Thermodynamic investigation of metamagnetism in pulsed high magnetic fields on heavy fermion superconductor UTe_2. *J. Phys. Soc. Jpn.* **88**, 083705 (2019).
73. Nakamine, G. et al. Superconducting properties of heavy fermion UTe_2 revealed by ^{125}Te-nuclear magnetic resonance. *J. Phys. Soc. Jpn.* **88**, 113703 (2019).
74. Ran, S. et al. Extreme magnetic field-boosted superconductivity. *Nat. Phys.* **15**, 1250–1254 (2019).
75. Bae, S. et al. Anomalous normal fluid response in a chiral superconductor UTe_2. *Nat. Commun.* **12**, 1–5 (2021).
76. Kittaka, S. et al. Orientation of point nodes and nonunitary triplet pairing tuned by the easy-axis magnetization in UTe_2. *Phys. Rev. Res.* **2**, 032014(R) (2020).
77. Metz, T. et al. Point-node gap structure of the spin-triplet superconductor UTe_2. *Phys. Rev. B* **100**, 220504(R) (2019).
78. Nakamine, G. et al. Anisotropic response of spin susceptibility in the superconducting state of UTe_2 probed with $^{125}\mathrm{Te}-$ NMR measurement. *Phys. Rev. B* **103**, L100503 (2021).
79. Paulsen, C. et al. Anomalous anisotropy of the lower critical field and Meissner effect in UTe_2. *Phys. Rev. B* **103**, L180501 (2021).
80. Ishizuka, J., Sumita, S., Daido, A. & Yanase, Y. Insulator-metal transition and topological superconductivity in UTe_2 from a first-principles calculation. *Phys. Rev. Lett.* **123**, 217001 (2019).
81. Xu, Y., Sheng, Y. & Yang, Y.-F. Quasi-two-dimensional fermi surfaces and unitary spin-triplet pairing in the heavy fermion superconductor UTe_2. *Phys. Rev. Lett.* **123**, 217002 (2019).
82. Miao, L. et al. Low energy band structure and symmetries of UTe_2 from angle-resolved photoemission spectroscopy. *Phys. Rev. Lett.* **124**, 076401 (2020).
83. Fujimori, S. et al. Electronic structure of UTe2 studied by photoelectron spectroscopy. *J. Phys. Soc. Jpn.* **88**, 103701 (2019).
84. Niu, Q. et al. Fermi-surface instability in the heavy-fermion superconductor UTe_2. *Phys. Rev. Lett.* **124**, 086601 (2020).
85. Shick, A. B. & E.,Pickett, W. Spin-orbit coupling induced degeneracy in the anisotropic unconventional superconductor UTe_2. *Phys. Rev. B* **100**, 134502 (2019).
86. Shick, A. B., Fujimori, S.-i & Pickett, W. E. UTe_2: a nearly insulating half-filled $j = \frac{5}{2} 5f^3$ heavy-fermion metal. *Phys. Rev. B* **103**, 125136 (2021).
87. Hiranuma, K. & Fujimoto, S. Paramagnetic effects of j-electron superconductivity and application to UTe_2. *J. Phys. Soc. Jpn.* **90**, 034707 (2021).
88. Shishidou, T., Gyeol, Suh, H., Brydon, P. M. R., Weinert, M. & Agterberg, D. F. Topological band and superconductivity in UTe_2. *Phys. Rev. B* **103**, 104504 (2021).
89. Fischer, M. H., Loder, F. & Sigrist, M. Superconductivity and local noncentrosymmetricity in crystal lattices. *Phys. Rev. B* **84**, 184533 (2011).
90. Chazono, M., Watanabe, H. & Yanase, Y. Superconducting piezoelectric effect. *Phys. Rev. B* **105**, 024509 (2022).
91. Watanabe, H., Daido, A. & Yanase, Y. Nonreciprocal optical response in parity-breaking superconductors. *Phys. Rev. B* **105**, 024308 (2022).
92. Watanabe, H., Daido, A., & Yanase, Y. Nonreciprocal Meissner response in parity-mixed superconductors. https://arxiv.org/abs/2109.14874 (2021).
93. Wadley, P. et al. Electrical switching of an antiferromagnet. *Science* **351**, 587–590 (2016).
94. Watanabe, H. & Yanase, Y. Symmetry analysis of current-induced switching of antiferromagnets. *Phys. Rev. B* **98**, 220412(R) (2018).

Acknowledgements

The authors are grateful to Jun Ishizuka, Hikaru Watanabe, and Shuntaro Sumita for helpful discussions. This work was supported by JSPS KAKENHI (Grants No. JP18H05227, No. JP18H01178, and No. JP20H05159) and by SPIRITS 2020 of Kyoto University. S.K. is supported by a JSPS research fellowship and by JSPS KAKENHI (Grant No. 19J22122).

Author contributions

S.K. and Y.Y. conceived the idea and initiated the project. S.K. performed the major part of the calculations. S.K. and Y.Y. discussed the results and co-wrote the paper.

Competing interests

The authors declare no competing interests.

Additional information

Supplementary information The online version contains supplementary material available at https://doi.org/10.1038/s42005-022-00804-7.

Correspondence and requests for materials should be addressed to Shota Kanasugi or Youichi Yanase.

Peer review information *Communications Physics* thanks Daniel Agterberg and the other, anonymous, reviewer(s) for their contribution to the peer review of this work. Peer reviewer reports are available.

Reprints and permission information is available at http://www.nature.com/reprints

Publisher's note Springer Nature remains neutral with regard to jurisdictional claims in published maps and institutional affiliations.